

# LOAN DOCUMENT

PHOTOGRAPH THIS SHEET

AD-A268 422



DTIC ACCESSION NUMBER



LEVEL

①

INVENTORY

AFOSR-TR-93-0543

DOCUMENT IDENTIFICATION

Feb 91

DISTRIBUTION STATEMENT A

Approved for public release  
Distribution Unlimited

DISTRIBUTION STATEMENT

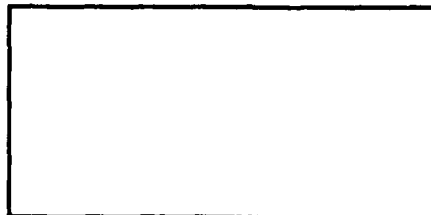
ACCESSION FOR	
NTIS	GRA&I
DTIC	TRAC
UNANNOUNCED	<input type="checkbox"/>
JUSTIFICATION	<input type="checkbox"/>
BY	
DISTRIBUTION/	
AVAILABILITY CODES	
DISTRIBUTION	AVAILABILITY AND/OR SPECIAL
A-1	

DISTRIBUTION STAMP

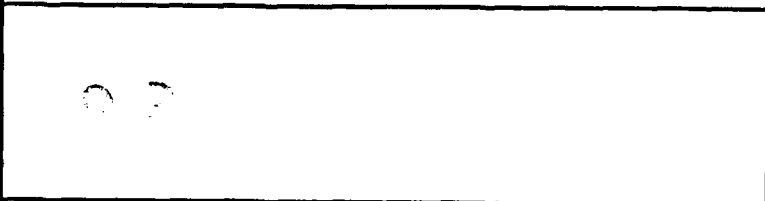
DTIC ELECTE  
S AUG 12 1993 D  
C

DATE ACCESSIONED

DTIC QUALITY INSPECTED 3



DATE RETURNED



DATE RECEIVED IN DTIC

93-18614



17.25

REGISTERED OR CERTIFIED NUMBER

PHOTOGRAPH THIS SHEET AND RETURN TO DTIC-FDAC

H  
A  
N  
D  
L  
E  
  
W  
I  
T  
H  
  
C  
A  
R  
E

9 3 0 0 2 3 2



TM-1479

AFOSR-TR- 03 05 43

**SUPERCONDUCTING MEISSNER EFFECT  
BEARINGS FOR CRYOGENIC TURBOMACHINES**

**Annual Technical Report**

**Contract No.: F49620-90-C-0007**

**Victor Iannello**

**CREARE INC.  
HANOVER, INC.**

**6761  
TM-1479  
FEBRUARY, 1991**

REPORT DOCUMENTATION PAGE			Form Approved OMB No. 0704-0188	
<small>Public reporting burden for this collection of information is estimated to average 1 hour per response, including the time for reviewing instructions, searching existing data sources, gathering and maintaining the data needed, and completing and reviewing the collection of information. Send comments concerning this burden estimate or any other aspect of this collection of information, including suggestions for reducing this burden, to Washington Headquarters Service, Directorate for Information Operations and Services, 1215 Jefferson Davis Highway, Suite 1204, Arlington, VA 22202-4302, and to the Office of Management and Budget, Paperwork Reduction Project (0704-0188), Washington, DC 20503.</small>				
1. AGENCY USE ONLY (Leave blank)	2. REPORT DATE 2/27/91	3. REPORT TYPE AND DATES COVERED Interim Report 11/1/89-12/31/90		
4. TITLE AND SUBTITLE "Superconducting Meissner Effect Bearings for Cryogenic Turbomachines"			5. FUNDING NUMBERS F49620-90-C-0007	
6. AUTHOR(S) V. Iannello			AFOSR-TR- 88 0543	
7. PERFORMING ORGANIZATION NAME(S) AND ADDRESS(ES) Create Inc. P.O. Box 71 Hanover, NH 03755			8. PERFORMING ORGANIZATION REPORT NUMBER TM-1479	
9. SPONSORING / MONITORING AGENCY NAME(S) AND ADDRESS(ES) Sponsored by: SDIO/IST Monitored by: AFOSR Bolling AFB, DC 20332-6448			10. SPONSORING / MONITORING AGENCY REPORT NUMBER NE DB82/F1	
11. SUPPLEMENTARY NOTES				
12a. DISTRIBUTION / AVAILABILITY STATEMENT Approved for public release; distribution unlimited.			12b. DISTRIBUTION CODE	
13. ABSTRACT (Maximum 200 words)  This report describes the first year efforts to develop a miniature, high speed superconducting bearing system suitable for cryogenic turbomachines such as miniature turboexpanders used in spaceborne cryocoolers for surveillance sensors. A bearing breadboard was designed, fabricated, and tested to a rotational speed of 450,000 rpm. Numerical models were developed to predict levitation focus between superconductors and permanent magnets, and validated with experimental data. The design of the turbomachine was initiated, including the conceptualization of a novel bearing system.				
14. SUBJECT TERMS			15. NUMBER OF PAGES 16	
			16. PRICE CODE	
17. SECURITY CLASSIFICATION OF REPORT	18. SECURITY CLASSIFICATION OF THIS PAGE	19. SECURITY CLASSIFICATION OF ABSTRACT	20. LIMITATION OF ABSTRACT U1	

## GENERAL INSTRUCTIONS FOR COMPLETING SF 298

The Report Documentation Page (RDP) is used in announcing and cataloging reports. It is important that this information be consistent with the rest of the report, particularly the cover and title page. Instructions for filling in each block of the form follow. It is important to *stay within the lines* to meet optical scanning requirements.

**Block 1. Agency Use Only (Leave blank).**

**Block 2. Report Date.** Full publication date including day, month, and year, if available (e.g. 1 Jan 88). Must cite at least the year.

**Block 3. Type of Report and Dates Covered.** State whether report is interim, final, etc. If applicable, enter inclusive report dates (e.g. 10 Jun 87 - 30 Jun 88).

**Block 4. Title and Subtitle.** A title is taken from the part of the report that provides the most meaningful and complete information. When a report is prepared in more than one volume, repeat the primary title, add volume number, and include subtitle for the specific volume. On classified documents enter the title classification in parentheses.

**Block 5. Funding Numbers.** To include contract and grant numbers; may include program element number(s), project number(s), task number(s), and work unit number(s). Use the following labels:

C - Contract	PR - Project
G - Grant	TA - Task
PE - Program Element	WU - Work Unit Accession No.

**Block 6. Author(s).** Name(s) of person(s) responsible for writing the report, performing the research, or credited with the content of the report. If editor or compiler, this should follow the name(s).

**Block 7. Performing Organization Name(s) and Address(es).** Self-explanatory.

**Block 8. Performing Organization Report Number.** Enter the unique alphanumeric report number(s) assigned by the organization performing the report.

**Block 9. Sponsoring/Monitoring Agency Name(s) and Address(es).** Self-explanatory.

**Block 10. Sponsoring/Monitoring Agency Report Number.** (If known)

**Block 11. Supplementary Notes.** Enter information not included elsewhere such as: Prepared in cooperation with...; Trans. of...; To be published in.... When a report is revised, include a statement whether the new report supersedes or supplements the older report.

**Block 12a. Distribution/Availability Statement.** Denotes public availability or limitations. Cite any availability to the public. Enter additional limitations or special markings in all capitals (e.g. NOFORN, REL, ITAR).

DOD - See DoDD 5230.24, "Distribution Statements on Technical Documents."  
 DOE - See authorities.  
 NASA - See Handbook NHB 2200.2.  
 NTIS - Leave blank.

**Block 12b. Distribution Code.**

DOD - Leave blank.  
 DOE - Enter DOE distribution categories from the Standard Distribution for Unclassified Scientific and Technical Reports.  
 NASA - Leave blank.  
 NTIS - Leave blank.

**Block 13. Abstract.** Include a brief (Maximum 200 words) factual summary of the most significant information contained in the report.

**Block 14. Subject Terms.** Keywords or phrases identifying major subjects in the report.

**Block 15. Number of Pages.** Enter the total number of pages.

**Block 16. Price Code.** Enter appropriate price code (NTIS only).

**Blocks 17. - 19. Security Classifications.** Self-explanatory. Enter U.S. Security Classification in accordance with U.S. Security Regulations (i.e., UNCLASSIFIED). If form contains classified information, stamp classification on the top and bottom of the page.

**Block 20. Limitation of Abstract.** This block must be completed to assign a limitation to the abstract. Enter either UL (unlimited) or SAR (same as report). An entry in this block is necessary if the abstract is to be limited. If blank, the abstract is assumed to be unlimited.



## LICENSE RIGHTS LEGEND

### GOVERNMENT PURPOSE LICENSE RIGHTS (SBIR PROGRAM)

Contract No. F49620-90-C-0007

Contractor: Creare Inc.

For a period of two (2) years after delivery and acceptance of the last deliverable item under the above contract, this technical data shall be subject to the restrictions contained in the definition of "Limited Rights" in DFARS clause at 252.227-7013. After the two-year period, the data shall be subject to the restrictions contained in the definition of "Government Purpose License Rights" in DFARS clause at 252.227-7013. The Government assumes no liability for unauthorized use or disclosure by others. This legend, together with the indications of the portions of the data which are subject to such limitations, shall be included on any reproduction hereof which contains any portions subject to such limitations and shall be honored only as long as the data continues to meet the definition on Government purpose license rights.



TABLE OF CONTENTS

LICENSE RIGHTS LEGEND.....	i
TABLE OF CONTENTS.....	ii
1 INTRODUCTION.....	1
2 THE NEED FOR MEISSNER BEARINGS IN MINIATURE CRYOGENIC TURBOMACHINES.....	2
3 PHASE II TECHNICAL OBJECTIVES AND APPROACH.....	3
4 SUMMARY OF TECHNICAL PROGRESS BY TASK.....	4
4.1 Task 1 - Fabricate and Test Meissner Bearing Breadboard.....	4
4.2 Task 2 - Develop Advanced Analytical Models.....	6
4.3 Task 3 - Design Turboexpander.....	8
4.4 Task 7 - Report and Manage.....	10
5 SUMMARY AND CONCLUSIONS.....	12
6 REFERENCES.....	12



## 1. INTRODUCTION

This Technical Progress Report covers the period of performance between November 1, 1990 and December 31, 1990 for our project entitled "Superconducting Meissner Effect Bearings for Cryogenic Turbomachines." This research is sponsored by the Innovative Science and Technology Branch of the Strategic Defense Initiative Organization (SDIO/IST), and managed by the Air Force Office of Scientific Research (AFOSR) under contract F49620-90-C-0007. The Air Force Program Manager is Dr. Harold Weinstock and the Principal Investigator is Dr. Victor Iannello. The period of performance for the contract is November 1, 1989 through October 31, 1991.

This program is aimed at the development of a Meissner bearing system for miniature high-speed cryogenic turbomachines for use in turbo-Brayton coolers. In Phase I, an analytical study for the proposed concept was performed which demonstrated its feasibility. The Phase II effort focuses on the design, fabrication, and testing of the Meissner bearing turbomachine. This report summarizes the technical progress for the year of the Phase II effort.



## 2. THE NEED FOR MEISSNER BEARINGS IN MINIATURE CRYOGENIC TURBOMACHINES

Spaceborne infrared sensors for surveillance and intelligence require cryogenic cooling to achieve high sensitivity levels and high signal to noise ratios. The importance of this data demands very high reliability of the cryogenic cooling system. Extended missions further require long cooling system operational lifetime. Additionally, the launch weight of the cryogenic cooling system directly impacts the cost per bit of intelligence data.

Cooling systems which rely upon boil off of liquid or solid cryogens from a dewar provide very high reliability and availability. Launch weight however is directly proportional to mission life in such systems, implying practical limits upon the useful life of spacecraft so equipped. Closed cycle mechanical cryocoolers are currently under development to provide reliable cooling for mission lengths beyond the practical limits of cryogen boil off (open) systems. State-of-the-art cryocoolers are currently under advanced development that use the turbo-Brayton thermodynamic cycle. These cryocoolers use hydrodynamic gas bearings for reliability and long life. For example, Creare is currently working on a 5 watt, 80 K single-stage cryocooler for NASA.

Cryocooler systems based on gas bearing turbomachines appear to have life and reliability issues well in hand, with reliability subject only to well established electronic system design and QA techniques. The key remaining issue concerns system efficiency, that is the cryocooler input power requirement per watt of refrigeration capacity at cryogenic temperatures. The input power requirement and heat radiator requirement strongly impact the system launch weight per unit of cooling capacity. All heat which conducts, or "leaks", to the cold end of the system must be lifted by cryocooler to radiator temperature for ultimate rejection. Each watt of heat leak penalizes the system with many additional watts of input power requirement, a situation of this escalating severity as sensor temperature are lowered.

Gas bearings employed in state-of-the-art cryocoolers need to run relatively warm, since their load bearing capacity relies upon temperature dependent gas viscosity. Every effort is therefore made in design to minimize the thermal conduction between the warm bearing zone and the cold expansion turbine. Small diameter turbine shafts are overhung as far as possible while still retaining adequately high critical speeds. Structural connections between the warm and cold ends are made as long and thin as possible while still retaining adequate structural stiffness and strength to resist launch loads. Nevertheless, the relative significance of heat leak varies inversely as machine size (cooling capacity), with the practical lower limit of acceptable efficiency for current turbo-Brayton machines occurring in the range of 3-5 watts.

Meissner effect bearings, which do not rely upon temperature dependent gas properties, promise significant improvements in small efficiency by virtue of running the bearings cold and reducing or eliminating the heat discussed above. With the replacement of state-of-the-art gas bearings with Meissner bearings, a large step can be taken towards increasing the performance of small cryogenic turbomachines. In Phase I we analytically showed that a 40% decrease in cryocooler input power can be achieved by incorporating Meissner bearings fabricated with currently available high temperature superconductor materials and fabrication techniques. These studies were performed for a 1 watt, 10 K cryocooler, where gas bearings for the coldest turboexpander were replaced with Meissner bearings.



### 3. PHASE II TECHNICAL OBJECTIVES AND APPROACH

The overall objective of Phase II is the development and demonstration of a turbomachine that employs Meissner bearings for radial support of the shaft. In Phase I, we determined that Meissner bearings are feasible for incorporation into turboexpanders. Based on the state-of-the-art analytical models presented in the literature, we showed that sufficient stiffness and damping can be generated for stable operation of the expander. Because Meissner bearings operate at cryogenic temperatures, we expect that a significant gain in thermodynamic performance can be achieved as compared to similar machines employing self-acting gas bearings because heat leak from the "warm" end of the shaft is virtually eliminated. We also have shown that present manufacturing techniques used for ceramic superconductors can be employed for our Meissner bearing design.

While the Phase I effort has demonstrated the feasibility of incorporating Meissner bearings into cryogenic turboexpanders, the Phase II effort focuses on the development of a prototype machine. The specific technical objectives of Phase II as stated in the Phase II proposal are:

- Fabricate a Meissner bearing test apparatus and generate data from which advanced analytical models can be developed and a final bearing design can be specified.
- Design and fabricate a prototypical turboexpander that incorporates Meissner bearings that can be used to provide refrigeration in a typical reverse-Brayton cryocooler.
- Test the turboexpander at cryogenic conditions to demonstrate the operability and performance gain afforded by the concept.

In order to meet these objectives the following seven task workplan is underway.

- |         |  |
|---------|--|
| Task 1. | Fabricate and test Meissner bearing breadboard |
| Task 2. | Develop advanced analytical models             |
| Task 3. | Design turboexpander                           |
| Task 4. | Fabricate turboexpander                        |
| Task 5. | Perform material degradation tests             |
| Task 6. | Test turboexpander                             |
| Task 7. | Report and manage                              |

This report documents the progress for the period November 1, 1989 through December 31, 1990 for Tasks 1, 2, 3, and 7, which were active for the reporting period.



#### 4. SUMMARY OF TECHNICAL PROGRESS BY TASK

##### 4.1 Task 1 - Fabricate and Test Meissner Bearing Breadboard

The scope of Task 1 is the design, fabrication, and high speed testing of a Meissner radial bearing. The objective is to gain experience with Meissner bearings in a short period of time and at a relatively small expense. To accomplish this, a simple breadboard has been fabricated and tested - a simple rotor disk-superconductor configuration to demonstrate rotational and surface speed prototypical of miniature turbomachines can be stably and repeatably achieved.

The simple disk rotor configuration is shown schematically in Figure 1. A cylindrical superconductor approximately 2.5 cm (1.0 in.) in diameter and height was supported in an insulated pool of liquid nitrogen ( $LN_2$ ). The YBCO superconductor was supplied to Creare by Catholic University, where it was fabricated from a melt-grown process developed by Dr. Hamid Hojaji of the Vitreous State Laboratory. (The quantitative characterization of this material was performed under Task 2.) The magnetic rotors for this configuration were rare-earth permanent magnet of cylindrical geometry. Both Nd-Fe-B and Sm-Co materials were tested.

In order to rotationally drive the rotor, two opposite nitrogen jets were tangentially directed at the surface of the magnet at diametrically opposite locations. The two jet configuration served to reduce the net radial jet force on the disk. Two techniques were explored to measure

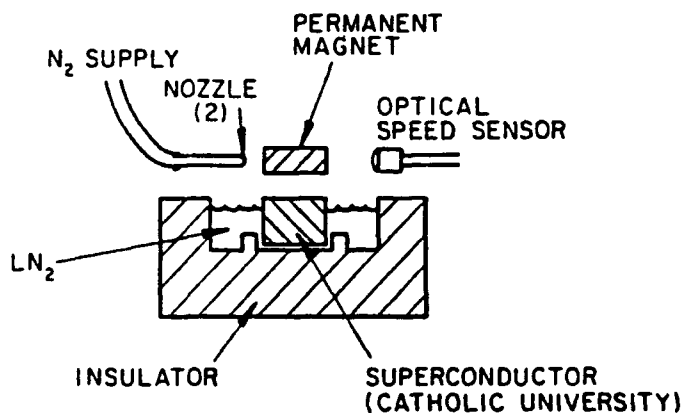


Figure 1. MEISSNER BEARINGS BREADBOARD

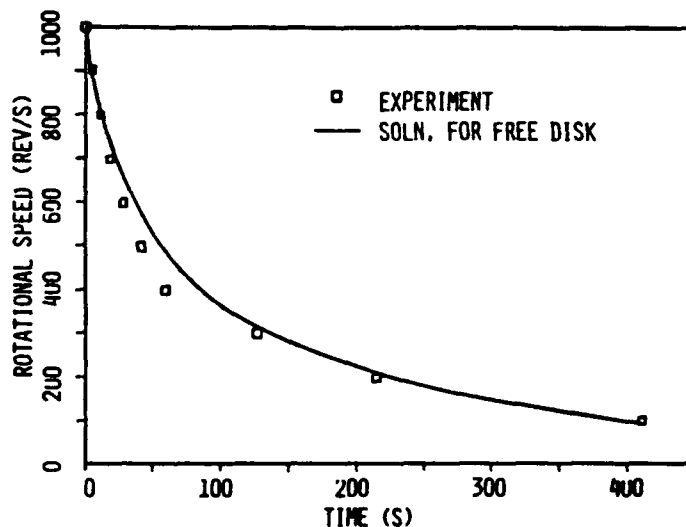


Figure 2. COASTDOWN CURVE FOR 2.5 CM ROTOR

the rotational speed. For the first, a timing mark was painted on the upper face of the rotor, and a strobe was used to determine the rotational speed. This technique was successfully used, but did not allow the determination of rotational speeds during spin-up and coastdown of the rotor. Instead, a timing mark was painted on the side of the disk, which was detected by an



optical sensor. The optical sensor combined the source light-emitting diode (LED) and photo detector in one package. The signal output from the photo detector was fed to conditioning electronics, and then to an oscilloscope, where the waveform consisted of a periodic series of spikes. The frequency of these spikes corresponded to the frequency of rotation of the rotor.

Using this setup, rotors with diameters between 2.5 and 25 mm (0.1 to 1.0 in.) were rotated to high speeds. In the first set of tests, a Nd-Fe-B rotor with dimensions 15 mm OD x 6.3 mm H (1.0 in. OD x 0.25 in. H) was spun to 60,000 rpm (1000 rev/s), which represented a surface speed of 80 m/s. Once at 60,000 rpm, the gas supplied to the nozzles was stopped, and the rotor coasted down. This coastdown is shown in Figure 2.

If the Meissner bearings are to be used for miniature turbomachines, it is important that the rotational drag they introduce is small compared to the other drag forces acting on the disk, such as windage (aerodynamic drag). To show this, the coastdown of a force disk subjected exclusively to windage was analytically predicted, and this result was compared to the experimentally observed coastdown.

The turbulent drag torque acting on both sides of a free-spinning disk is given by [1]

$$2M = 0.073 \rho \omega^2 R^5 (\nu/\omega R^2)^{0.2} \quad (1)$$

where  $\rho$  is the fluid density,  $\omega$  is the angular velocity,  $R$  is the disk radius, and  $\nu$  is the kinematic viscosity. The coastdown of the disk is governed by

$$2M = I\dot{\omega} \quad (2)$$

where  $I$  is the moment of inertia of the disk (which equals  $MR^2/2$ ). After combining (1) and (2), solving for  $\dot{\omega}$ , and integrating, the following coastdown curve is obtained:

$$\omega = \left[ \frac{1}{\frac{1}{\omega_0^{0.8}} + \beta t} \right]^{1.25} \quad (3)$$

where  $\beta = 0.058 \rho R^{4.6} \nu^{0.2} / I$  and  $\omega_0$  is initial angular velocity.

Figure 2 compares the analytical windage with the experimental coastdown curves. The agreement is satisfactory for the seven minute coastdown. We conclude, therefore, that the superconductor imports little additional drag on the rotor.

Further testing was performed with smaller rotors to demonstrate stability at ultra-high rotational speeds. A 6.4 mm (0.25 in.) rotor was spun to a rotational speed of 450,000 rpm (7500 rev/s), which represents a surface speed of 150 m/s. This surface speed far exceeds that required by the turboexpander application (about 90 m/s). We are not aware of a faster spinning rotor supported on Meissner bearings.



## 4.2 Task 2 - Develop Advanced Analytical Models

The scope of Task 2 is the development of sound design methods that allow us to gain insight and optimize the configuration of the Meissner bearings for maximum levitation force and stiffness. To accomplish this, analytical models are being developed based on first principles with constitutive relations for superconductor properties such as the current density  $J_c$ . The model is being compared with experimental force data obtained here.

A one-dimensional magnetization model was first developed to predict the net magnetization of a superconductor when subjected to an external field. Magnetization curves are often known for a superconductor sample from magnetometer measurements, but critical current densities are often not known because of the experimental difficulty of taking the measurement. The 1D model therefore provides a simple method for "backing out" the current densities when otherwise not known.

The magnetization model is based on Bean's critical state model, which assumes currents in the superconductor are either at their critical density at a given location or are not flowing. The field in the superconductor is thus given by

$$\frac{dB}{dx} = \mu_0 J_c \quad (4)$$

where  $B$  is the magnetic field and  $\mu_0$  is the permeability of free space. In the Bean model,  $J_c$  is assumed constant so that  $B$  changes linearly in the superconductor. Here, we allow  $J_c(B)$ , which more accurately represents HTSCs.

Figure 3 compares the experimental and calculated magnetization curves for a 1.3 mm thick superconductor when the external field is applied along the  $c$ -axis (conduction in the  $a$ - $b$  plane). The YBCO sample was fabricated and magnetically characterized by Catholic University. It was found that excellent agreement between the experiment and calculations could be obtained with  $J_c$  given by

$$J_c = J_0 e^{-|B/B_0|} + J_1 e^{-|B/B_1|} \quad (5)$$

and  $J_0 = 1600 \text{ A/cm}^2$ ,  $B_0 = 0.1 \text{ T}$ ,  $J_1 = 3760 \text{ A/cm}^2$ , and  $B_1 = 100 \text{ T}$ . The local magnetic flux densities in the superconductor are shown in Figure 4 for various points on the magnetic hysteresis curves.

A 2D numerical code was next developed to predict the force between permanent magnets and superconductors in arbitrary geometries. At the heart of this numerical code is Maxwell's Equations field solver for the vector potential,  $A$ , defined by  $\mathbf{B} = \nabla \times \mathbf{A}$ .

The permanent magnet is modeled as equivalent surface currents necessary to produce an identical volume magnetization. This assumption assumes uniform magnetization of the magnet (which is valid for rare-earth magnets). The magnet model also includes the demagnetization curve of the hard magnetic material so that the field produced by the magnet is a function of the net reluctance of its environment.

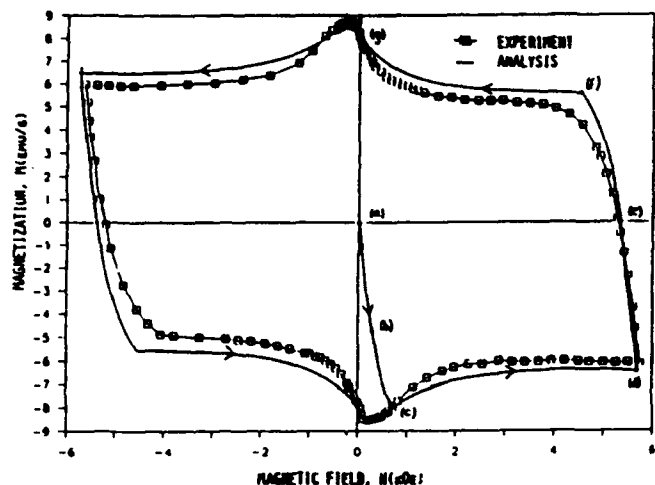


Figure 3. CALCULATED AND MEASURED MAGNETIZATION CURVES FOR A 1.3 MM THICK MELT-GROWN SUPERCONDUCTOR

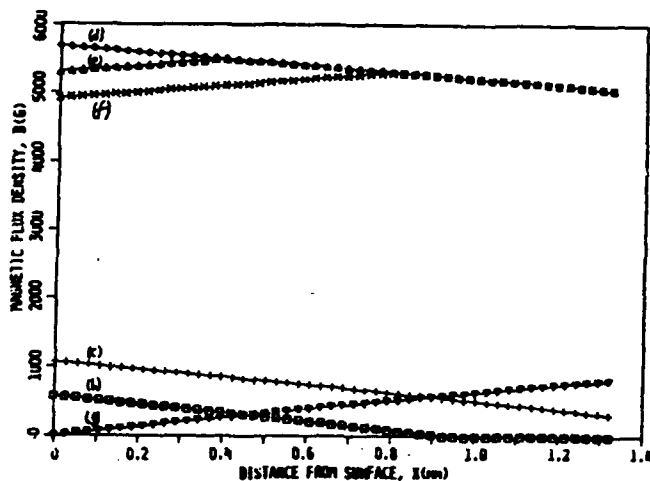
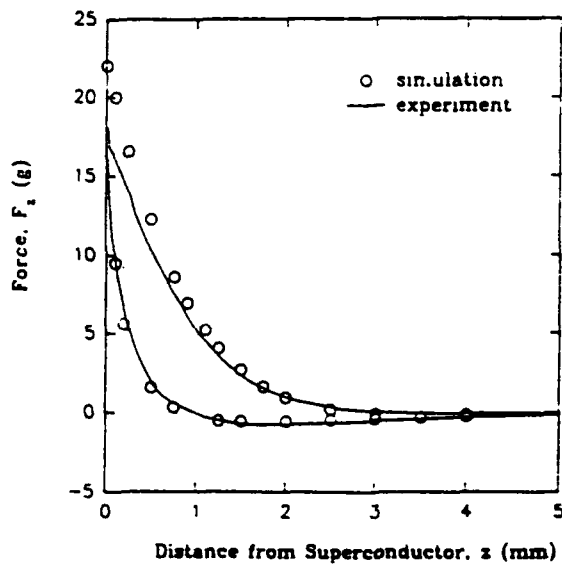


Figure 4. MAGNET FIELD IN A 1.3 MM THICK MELT-GROWN SUPERCONDUCTOR

The superconductor is treated according to the critical-state model. In this model, the persistent currents that shield the interior from the applied magnetic fields have a current density equal to the critical current density  $J_c$ . The penetration of the magnetic field into the superconductor occurs as follows. Initially, the flux density  $B$  equals zero inside the superconductor. On the application of an external field, a shielding current develops in a thin layer on the superconductor surface. If the current density is greater than  $J_c$  in this layer, the layer goes normal, i.e., has a finite resistivity and therefore a finite electric field. The presence of the electric field accelerates electrons in the superconductor adjacent to this layer so that the current carrying layer (and magnetic flux) penetrates deeper into the superconductor. This process stops only when the current carrying layer expands sufficiently for the shielding current density to fall just below  $J_c$ . Then, instantaneously, the electric field vanishes and the shielding current flows persistently at  $J_c$  in the superconductor region it has penetrated.

Once the magnetic field and current densities within the superconductor are known, the Lorentz forces can be calculated in a relatively straightforward manner. Figure 5 compares the experimental force data with the numerical prediction for a 2.5 mm (0.1 in.) cylindrical magnet above a melt-grown superconductor supplied to us by Catholic University. The only constitutive relations used were the demagnetization curve of the magnet as supplied to us by the magnet vendor, and the critical current density of the superconductor (Eq. 5). As shown in the figure, the agreement is excellent except at small magnet-superconductor spacings. The setup used to obtain the experimental data is shown in Figure 6.



**Figure 5. LEVITATION FORCE FOR 25MM MAGNET ABOVE A MELT-GROWN SUPERCONDUCTOR-COMPRESSOR OF MODEL AND EXPERIMENT**

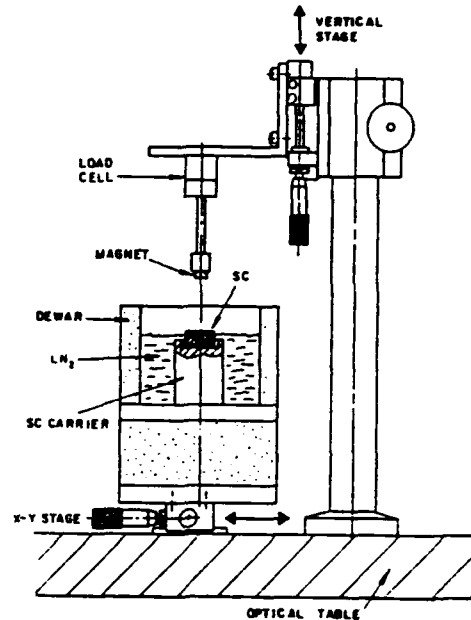


**Figure 6. EXPERIMENTAL SETUP FOR FORCE DATA**

### 4.3 Task 3 - Design Turboexpander

The objective of this task is to develop a mechanical design for the miniature turbomachine. The challenging element of this task is to design a Meissner bearing system that precisely positions the shaft so that small running clearances are possible in the turbine, resulting in low leakage rates around the turbine blade passages. Another challenge is the development of a means to support the shaft while the superconductor is cooled below its critical temperature ( $T_c$ ). Because of the hysteretic nature of Type II superconductors, a range of equilibrium positions for the shaft exists. A shaft that starts off in mechanical contact with a non-rotating member must therefore be lifted off by some other means, be it manually or otherwise. In the past, this has limited Meissner bearings for use in laboratory demonstrations and basic research devices. As such, the bearing has little practical use.

We have improved our superconducting bearing to remove this limitation. By employing a special configuration of permanent magnets and supplying the bearing with a small supply of gas, the shaft may stably be and precisely positioned at all times.

The bearing designed under this task offers the following advantages over other passive superconducting bearings. It:

- Precisely and non-mechanically positions the rotating shaft while the superconducting material passes from its normal to superconducting state, thereby "pinning" the magnetic flux such that the shaft is "cradled" in a very precise position.
- Can support steady loads, even when the superconductor exhibits "flux creep".



- Allows operation of the superconductor in the hysteric Type II regime, where superconductor-magnet forces are highest.
- Provides load capacity and stiffness, even when the superconducting materials are at temperatures above their critical temperatures and are therefore not superconducting.
- Does not require precision machining of the superconducting material.
- Allows the gap between the permanent magnets and the superconducting materials to be minimized, thereby increasing the stiffness, load capacity, and damping of the bearing.

The improved bearing is shown in Figure 7. The bearing system consists of permanent magnets in the bore of the shaft; stationary permanent magnets of annular shape which encircle the shaft; superconducting materials at the shaft ends in very close proximity to the shaft magnets; and a duct and pinhole outlet which direct a flow of gas towards one shaft end. As shown in Figure 7, the turbine may be located midway between the bearings.

When the superconductor materials are above their critical temperature and are therefore not superconducting, the stationary permanent magnets interact with the permanent magnets in the shaft to radially position the shaft. With the magnet polarities as shown, the magnet configuration will center the shaft in the stationary permanent magnets due to radial repulsive forces between poles of the same polarity. The shaft is stably supported along its radial axes.

The permanent magnet interaction also produces an unbalance axial force on the shaft so that the permanent magnet suspension is by itself unstable (in accordance with Earnshaw's Theorem). In order to produce stability, a gas jet is directed towards one end of the shaft. The position of the stationary magnets can be chosen to produce a net magnetic force towards the gas jet. This net force is exactly balanced by the force of the gas jet on the shaft. Because the gas jet imparts a force on the shaft with an axial stiffness much greater than the "negative" (unstable) stiffness produced by the permanent magnet, the shaft is stably positioned without mechanical contact. In this suspended position, the shaft may rotate freely about its axial axis.

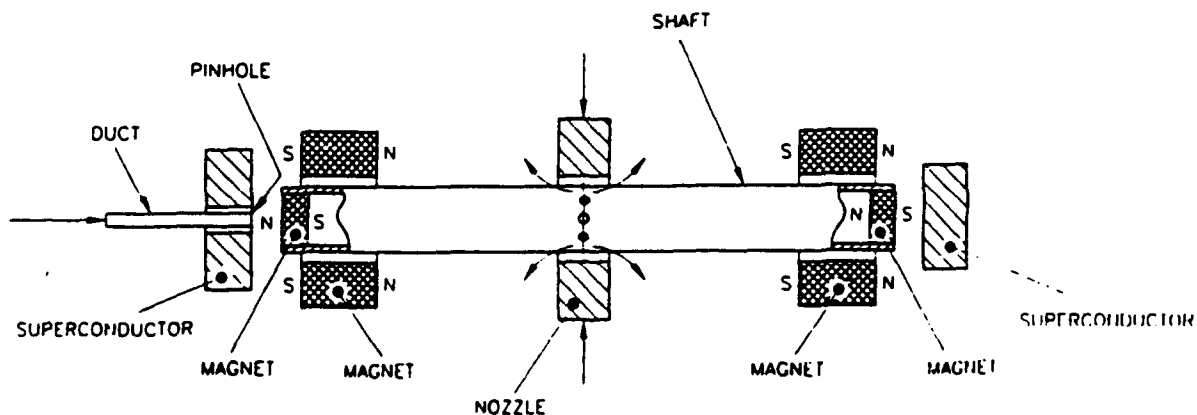


Figure 7. IMPROVED MEISSNER BEARING SYSTEM



As the superconductors are cooled below their transition temperature, the magnetic flux produced by the permanent magnets that penetrate the superconductor is "pinned". Any change in position of the shaft will induce supercurrents in the superconductor which will tend to resist the change in position. As a result, the shaft will be "cradled" in the desired shaft position. The superconductor-magnet interaction generates a restoring force as the shaft is transversely displaced in any direction away from its equilibrium position. This interaction, however, does not resist shaft rotation, due to the azimuthal symmetry of magnetic field produced by the permanent magnets. The rotational drag can thus be made quite small.

It might appear that the superconductors are not necessary since the permanent magnets and gas jet alone are sufficient for positioning the shaft. In fact, the superconductors greatly add to the stiffness and damping of the bearing system. Without the superconductors, the bearing would have insufficient stiffness and damping for high speed rotation of the shaft.

Flux creep, or a decay of supercurrent amplitude with time, has been experimentally observed in high temperature superconductors. If a magnet that is "pinned" in a certain position is subsequently displaced, the restoring force generated by the induced currents will initially be high, and then will decay with time. By incorporating the stationary permanent magnets into the bearing system, the bearing will support steady loads even with superconductor flux creep.

Because the interaction between a superconductor and a permanent magnet is maximized at close spacings, the improved bearing offers the advantage of precisely positioning the shaft in close proximity of the superconductor. As a result of the small gap spacing between the superconductor and the face of the permanent magnets in the shaft, the stiffness, damping, and load capacity of the bearing are maximized.

The bearing also offers certain fabrication advantages over other passive superconducting bearings. The superconductor need not be specially contoured or machined. The face of the superconductor need only be ground flat.

A simple model of the improved bearing system was built and tested at room temperature to demonstrate its positioning and stability characteristics. The bearing performed as designed. In the next (fifth) quarter, a dummy shaft incorporating permanent magnets will be balanced, and the bearing test rig will be brought to a liquid nitrogen temperature, and the stability at high substantial speeds will be explored.

#### **4.4 Task 7 - Report and Manage**

This task covers general project planning, monitoring, and status reporting activities. As specified in the program contract, two reports are the required deliverables - an Annual Technical Progress Report and the Final Report. This report is the first of these reports.

Creare staff has also prepared for and attended three meetings for and with government officials. The first meeting was held November 17, 1989 in Washington, DC. Creare presented an overview of this program and delivered presentation materials, MTG-89-11-233.

The second meeting was held April 4, 1990, at NASA Goddard Space Flight Center. Creare presented the accomplishments of this program achieved at that time, and delivered presentation materials, MTG-90-3-271.



The third meeting was held in Washington DC, on October 31, 1990. The meeting was attended by government officials from SDIO, DARPA, and AFOSR. The Principal Investigator at this meeting presented recent accomplishments of this program, and delivered MTG-90-10-328.

A patent disclosure was also prepared under this task. The patent disclosure discusses the novel features of the improved Meissner bearing that was designed under Task 3, and was delivered to the Program Manager on October 21, 1990.



## 5. SUMMARY AND CONCLUSIONS

This technical report documents the progress made between November 1, 1989 and December 31, 1990, for the program entitled "Superconducting Meissner Effect Bearings for Cryogenic Turbomachines." The main accomplishments for the first year of the program were:

- Demonstration of Meissner bearing concept at a surface speed of 150 m/s and a rotational speed of 450,000 rpm.
- Quantification of drag torque on a rotor supported in Meissner bearings.
- Development of a magnetization numerical model to predict the magnetic hysteresis curves of 1D superconductors.
- Development of a 2D numerical model that solves Maxwell's in the presence of superconductors and permanent magnets.
- Extension of 2D model to predict levitation forces and current densities.
- Comparison of 2D model with experimentally obtained force data.
- Conceptualization of a novel bearing system that can be used in "real" turbomachine and provides support at room temperature.
- Demonstration of novel bearing system at room temperature.

Work is currently underway to test the improved bearing at cryogenic temperatures. Once this aspect of the turbomachine design has been verified, the balance of the turbomachine will be designed, fabricated, and tested in the second year of the program.

## 6. REFERENCES

1. Schlichting, H.; Boundary Layer Theory, McGraw-Hill, 1979, pp. 647-649.